ACS Partner Journal

Journal of the American Society for Mass Spectrometry

pubs.acs.org/jasms

Article

Probing the Interactions of Cytochrome c with Anionic Phospholipid Nanodiscs Using Millisecond Hydrogen–Deuterium Exchange Mass Spectrometry

Vimanda Chow, Cristina Lento, and Derek J. Wilson*

Cite This: J. Am. Soc. Mass Spectrom. 2025, 36, 1052–1059

Read Online

ACCESS | Metrics & More | Article Recommendations | Supporting Information

ABSTRACT: The interplay between the anionic phospholipid cardiolipin (CL) and cytochrome c (cyt c) holds significance in the early stages of apoptosis. Despite identification of up to four potential sites of interaction between cytochrome c and cardiolipin bearing membranes, the exact mode of interaction remains unexplained, especially given that some of the putative binding surfaces are mutually exclusive. In this study, we utilize millisecond time-resolved electrospray ionization hydrogen–deuterium exchange mass spectrometry (TRESI-HDX-MS) to investigate conformational and dynamic changes in cytochrome c in the presence of various phospholipids (DMPC, POPG, and CL) incorporated into nanodiscs. We observe that, among the proposed binding sites, the adjacent "L"- and "A"-sites exhibited a decrease in deuterium exchange, while the "N" site remained unperturbed, suggesting a specific orientation of cytochrome c with respect to cell membranes upon binding. We also demonstrate that negatively charged phospholipids with physical differences (*i.e.*, POPG and CL) exhibit essentially the same interaction with cytochrome c, supporting the utility of POPG nanodiscs as a model for cytochrome c–membrane interactions.

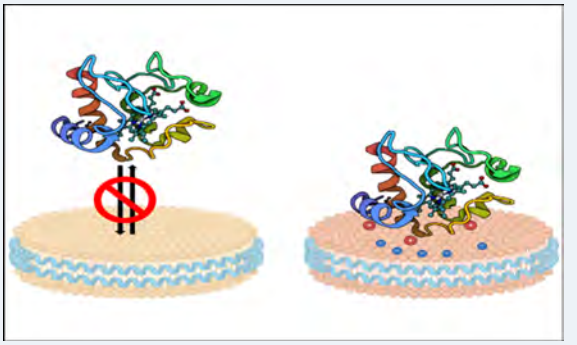

INTRODUCTION

Proteins can undergo various changes in their structural conformation, depending on pathological and physiological processes within the cell. Therefore, it is essential to understand the shifts in structure and conformational dynamics proteins undergo to perform their biological functions. Cytochrome c (cyt c) is a common "model" protein that plays crucial roles in the mitochondrial respiratory chain and the early steps of cell apoptosis.[1−4] Under normal cell conditions, cyt c has been well characterized as a shuttle that transfers electrons from cyt c reductase (complex III) to cyt c oxidase (complex IV). Once the cell experiences stress, it may undergo the early stages of apoptosis, where cyt c acts as a peroxidase, resulting in the oxidation of cardiolipin, altering the fluidity of the inner mitochondrial membrane. The disruption in the normal packing of lipids within the membrane, results in the release of cyt c into the cytosol where apoptosomes are formed leading to cell death.[2,3,5−7] Over the past decade, many researchers have studied the involvement of cytochrome c in the early stages of apoptosis, where it undergoes a conformational change that converts it from electron carrier to active peroxidase.[8,9] This process is relevant for disease interventions, particularly in the wide range of pathologies involving cells that become insensitive to apoptotic signaling.[6,8]

In healthy cells, cyt c is a 12 kDa heme protein located in the inner mitochondrial membrane, where 15% is bound to an anionic phospholipid headgroup, cardiolipin (CL). The other 85% is free or loosely bound to the membrane via electrostatic interactions.[8,10,11] Upon cell stress, cyt c forms a complex with CL through four particular interaction sites: A-site, L-site, N-site, and C-site (Figure 1).[1,6,8,11] Upon complexation, cyt c unfolds into a non-native conformation that acts primarily as a peroxidase.[6,8,12,13] Although the physiology of cyt c has been understood for more than half a century, the mechanisms of cyt c/CL complex formation have remained underexplored and, where information is acquired, contentious.

There exists a degree of agreement in that the interaction is initially charge-driven, with positively charged amino acid residues of cyt c interacting electrostatically with the negatively charged phospholipid headgroups of the membrane.[2,7−9,14,15] Among the potential binding sites, it has been suggested that the A-site initiates complex formation through interactions involving Lys72, Lys63, Lys86, and Lys87 as key residues, followed by additional contacts within the C-site (Figure 1A).[8,15] The A-site interactions are thought to be primarily

Received: November 29, 2024
Revised: March 20, 2025
Accepted: March 25, 2025
Published: April 2, 2025

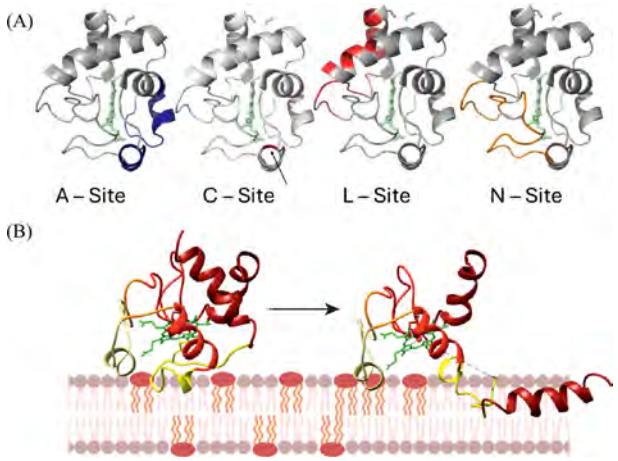

Figure 1. (A) Structural models (PDB 1HRC) showing proposed sites of interaction between cytochrome c and phospholipid membranes, corresponding to the A-site (T49–K55, N70–I81), the C-site (N52), the L-site (V3–K27, Y97–A101), and the N-site (E21–Y48, K53). (B) A proposed model for cytochrome c phospholipid interactions with structural changes, adapted from ref 6 under creative commons attribution license, copyright 2020 Antonio Díaz-Quintana et al.

electrostatic, while the C-site is involved in hydrogen bonds and potentially hydrophobic interactions (through insertion of a lipid tail into the hydrophobic cavity of cytochrome c).[14,16,17] Another positively charged patch of residues, the L-site, has been proposed to be involved in complex formation, specifically Lys22, Lys25, His26, Lys27, and His33 (Figure 1A).[8,18] In addition, the fourth binding site, N-site, was recently discovered via NMR to participate in the binding of liposomes to mediate membrane fusion (Figure 1A).[3,6,8]

There is a long-running debate as to whether all four of these binding sites are directly involved in the interaction with CL, particularly the C and L sites. Among those who have studied structural changes that occur when cyt c interacts with CL liposomes, C-site and L-site binding are observed under highly acidic conditions (pH 2.6) and slightly below pH 7, respectively.[18,19] Since C-site binding is thought to be relevant only at low pH, and we do not observe unexpected evidence for it in this (physiological pH) study, we have omitted it from the discussion. However, from a biological perspective, as the local cell environment changes pH during the electron transport chain, different structural conformations of cyt c are present, making all other binding sites at least potentially relevant.[1,6,11]

There is also substantial debate around cyt c undergoing significant structural changes following complexation with CL membranes. Some have proposed that cyt c undergoes a two-step unfolding event where the His26-Pro44 hydrogen bond breaks, leading to tertiary unfolding at the N- to C-termini and peroxidase activity-associated M80-heme coordination (Figure 2).[9] Multiple studies have shown that forming the cyt c/CL complex leads to a broad unfolding of the tertiary structure necessary for peroxidase activity.[9,20,21]

Among the few proposed specific structural models for phospholipid binding, the lipid anchoring model, which holds that one or two acyl chains of CL protrude out of the membrane and is/are inserted into a hydrophobic cavity of the protein (driving the "misfolding" of cyt c into its peroxidase configuration), is likely the most widely promoted. In particular, it has been argued that this occurrence may be necessary for CL-oxidation, which is a hallmark of apoptosis.[1,12,21,22] Nonetheless, it can be argued that this model would involve an exceptionally high free energy barrier for "flipping" of the acyl chain(s).[16]

Currently, all published studies looking at the structural changes of cyt c utilize CL-liposomes or unilamellar vesicles. Although these often provide a suitable bilayer membrane mimic, for peripheral membrane proteins in particular, the interaction with the curved bilayer and surrounding solution can affect the interaction between protein and phospholipid headgroups.[6,23] Therefore, it is essential to consider if the membrane mimic used is representative or if it ignores the interaction between the bilayer and the relationship with the membrane.[24] Specific to the formation of the cyt c- CL complex, Elmer-Dixon et al. (2020) along with other studies showed that the curvature of liposomes might provide structural information that may not be physiologically relevant as the surface of the inner mitochondrial membrane (IMM) is concave, while the majority of the aforementioned studies measure binding to the convex outer surface of the CL liposome.[7,25] Mohammadyani et al. (2018) used coarse-grained molecular dynamics modeling to validate that CL presence in the eukaryotic mitochondrial and bacterial membranes induces a negative curvature.[3] In this study, we use nanodiscs, which provide a more organized, controlled, and "flat" membrane mimic. We aim to characterize the structure and dynamics of cyt c in its "unbound" configuration (absent of phospholipids nanodiscs) compared to the "bound" configuration using millisecond hydrogen–deuterium exchange mass spectrometry (HDX-MS). HDX-MS measures which regions of the protein become more or less protected from solvent exchange upon complexation, resulting either from intermolecular interactions or rearrangement of the intramolecular hydrogen bonding network.[26] Using short HDX labeling time points (milliseconds to seconds) allows for the detection of changes in the structure of weak (or fast cycling) binding interactions or subtle shifts in conformation.[26]

EXPERIMENTAL SECTION

Protein Purification. MSP1D1 was expressed and purified from *E. coli* BL21-CodonPlus (DE3) cells containing the pET28a-MSP1D1 vector (Addgene). The protein purification process is described in detail by Oganesyan et al. (2021).[27] In short, the sonicated supernatant postlysis was purified using Ni^{2+} affinity gravity chromatography with three washes of increasing concentration of imidazole followed by an elution buffer using 0.4 M imidazole. The protein was concentrated to 4 mg/mL and stored in 20 mM Tris/HCl, 100 mM NaCl, and 1 mM EDTA buffer pH 7.0 with 25% glycerol at −80 °C for future use. This particular length of MSP1D1 produces nanodiscs with a diameter size of 10 nm, which is acceptable for cyt c with a diameter of 3.4 nm.[5]

Production, Purification, and Validation of Nanodiscs. Nanodiscs were made according to established protocols.[28–30] For this study, four types of lipid constituents for nanodiscs were used: 100% 14:0 DMPC (1,2-dimyristoyl-*sn*-glycero-3-phosphocholine, Avanti Polar Lipids cat no. 850345P) as the negative control, 100% 16:0–18:1 POPG (1-palmitoyl-2-oleoyl-*sn*-glycero-3-phospho-(1′-rac-glycerol) (sodium salt), Avanti Polar Lipids cat no. 840457P) as the positive control, 100% 18:1 CL (1′3′-bis[1,2-dioleoyl-*sn*-glycero-3-phospho]-glycerol (sodium salt), Avanti Polar Lipids

https://doi.org/10.1021/jasms.4c00478
J. Am. Soc. Mass Spectrom. 2025, 36, 1052–1059

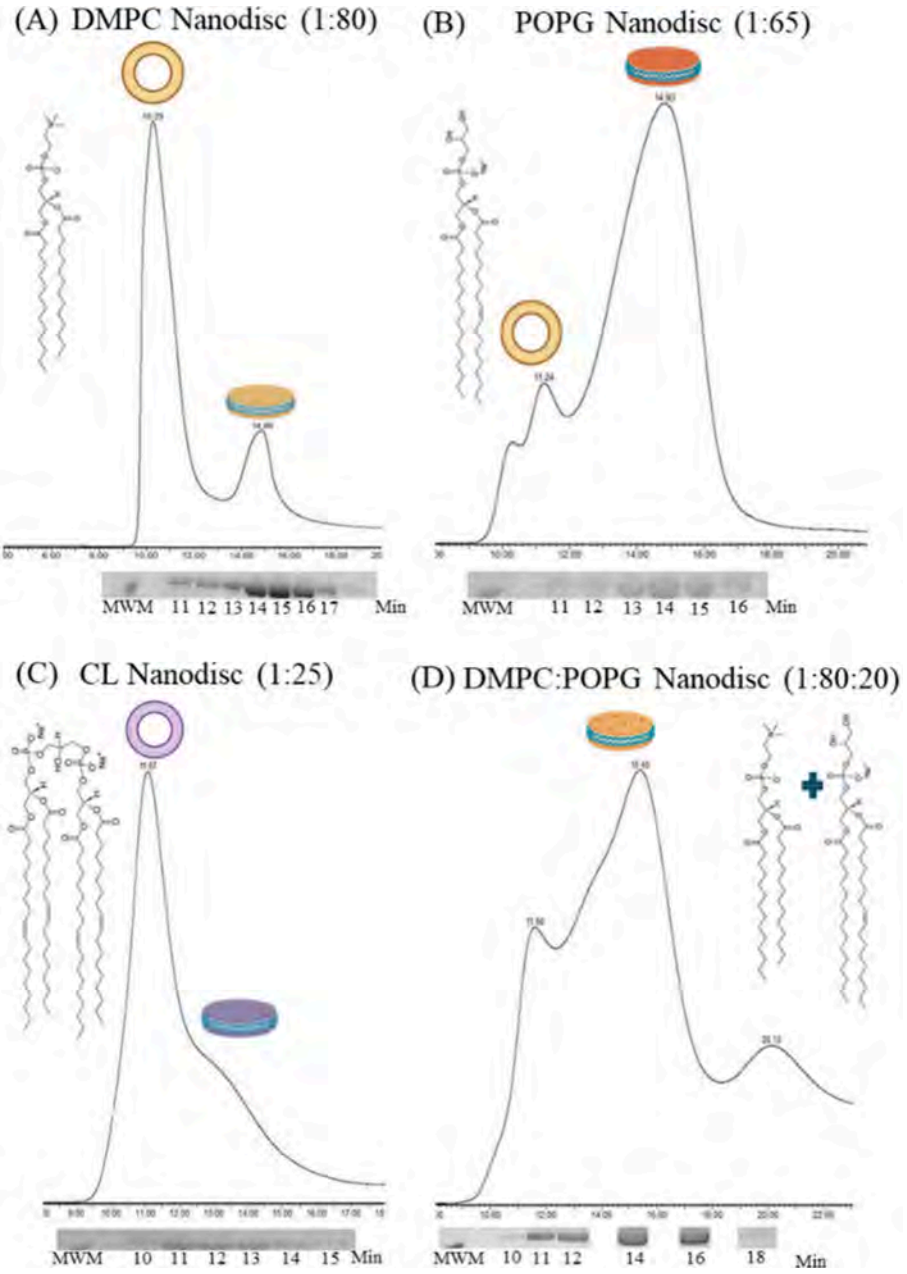

Figure 2. Size-exclusion chromatography with corresponding SDS-PAGE protein bands of prepared nanodiscs. (A) 1,2-Ditetradecanoyl-*sn*-glycerol-3-phosphocholine DMPC 14:0 nanodiscs, (B)1-exadecanoyl-2-(9Z-octadecenoyl)-*sn*-glycero-3-phospho-(1′-rac-glycerol) (sodium salt) 16:0/18:1 POPG nanodiscs, (C) cardiolipin CL 18:0 nanodiscs, and (D) mixture of 80%DMPC and 20% POPG nanodiscs. The chemical formulas of DMPC, POPG, and CL are displayed in each panel A−C. Samples were run on a Superdex 200 prep grade column (300 mm × 7.8 mm), monitoring absorbance at 280 nm. SDS-PAGE gels are displayed under the respective chromatograms corresponding to fractions collected. The molecular weight marker (MWM) band corresponds to the 25 kDa standard (Thermofisher, cat no. 26620).

cat no. 710335P), and 80:20 DMPC:POPG. All nanodiscs were formed using MSP1D1 as the membrane scaffolding protein. First, DMPC and POPG lipids were suspended in HPLC-grade water to a final concentration of 200 mM, diluted further in 100 mM sodium chlorate, and sonicated in a heat bath until the lipid solution appeared clear. The lipid-to-MSP ratio was calculated where the ratios for DMPC, POPG, CL, and DMPC:POPG are 1:80, 1:60, 1:25, and 1:80:20, respectively. Nanodiscs containing DMPC lipids were first incubated at its transition temperature at room temperature (transition temperature is 25 °C) for 20 min and then at 4 °C for 1 h, and POPG lipids (transition temperature is 4 °C) were incubated at 4 °C for 1 h before incubation with biobeads SM Absorbents (Biorad, cat no. 152-8920). DMPC was incubated with biobeads for 2 h at 4 °C, while POPG required 4 h at 4 °C. For the formation of CL nanodiscs, the following protocol provided the best results: 5 mg of CL lipids was resuspended in 20 mM HEPES buffer, pH 7.2, and sonicated until transparent before adding 2 mg of MSP1D1 to a final volume of 1.5 mL. The transition temperature of CL is ∼50 °C; therefore, the sample was then incubated in a 48−50 °C water bath until the solution appeared clear with no visible lipid particles.

Size exclusion chromatography (SEC), SDS-PAGE, and nuclear magnetic resonance (NMR) were used for nanodisc

https://doi.org/10.1021/jasms.4c00478
J. Am. Soc. Mass Spectrom. 2025, 36, 1052−1059

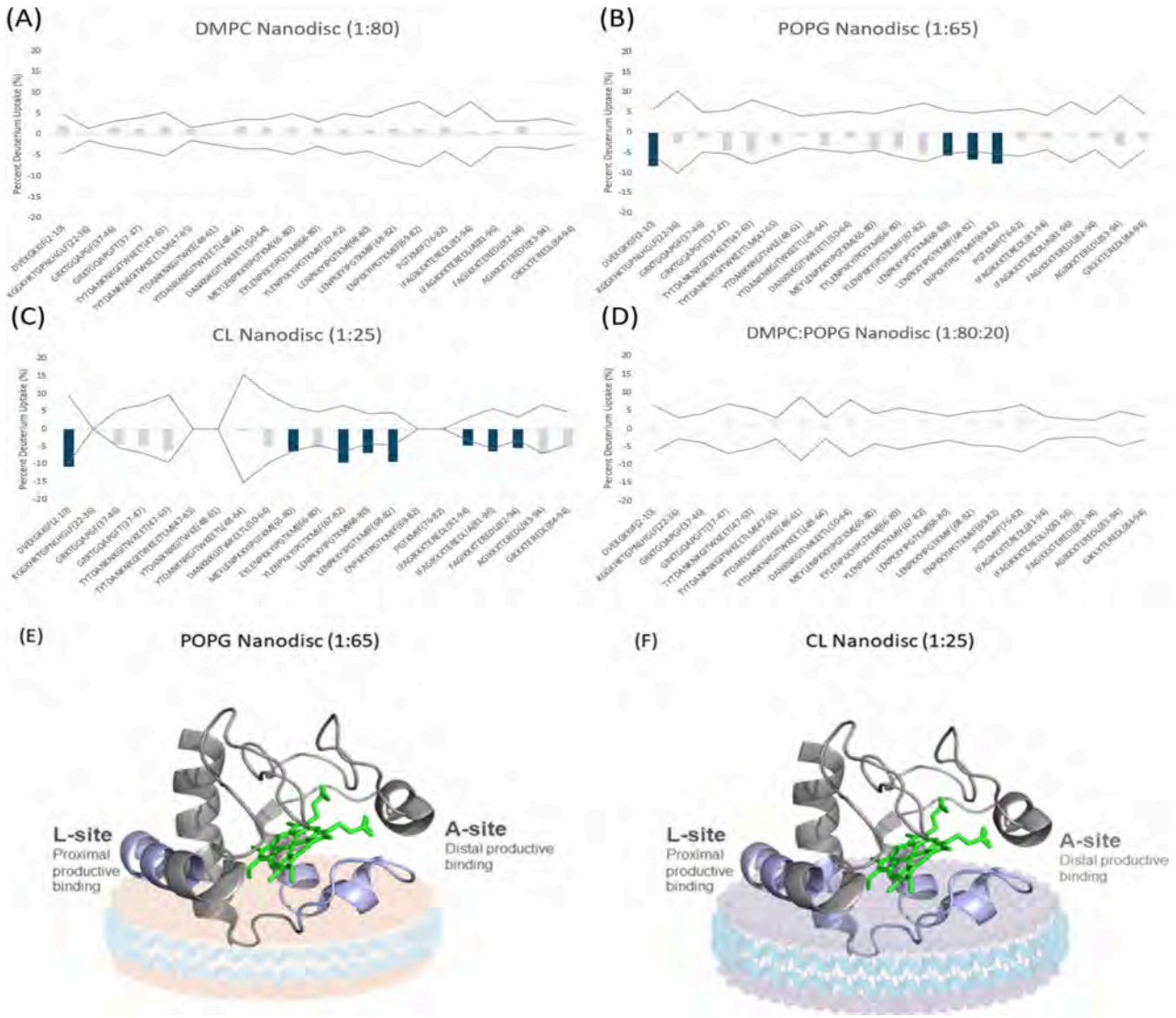

Figure 3. Summed difference plots of % deuterium uptake of the complex with nanodiscs and cyt c. (A) HDX difference plot of cyt c in the presence of DMPC nanodiscs, (B) HDX difference plot of cyt c in the presence of POPG nanodiscs, (C) HDX difference plot of cyt c in the presence of CL nanodiscs, and (D) HDX difference plot of cyt c in the presence of 80:20 DMPC: POPG nanodiscs. (E and F) Structural visualization of the interaction between the A- and L-site of cyt c (PDB: 1HRC) and the nanodisc surface. Statistically significant decreases in deuterium uptake upon complexation are depicted by the colored bars, with a significance determined by a threshold for each peptide (2σ, $n = 4-12$). The gray-colored bars displays nonstatistically significant changes between the bound and unbound states. To be considered statistically significant, the ΔHDX must exceed the gray line, which is two times the summed propagated error.

purification and validation. Nanodiscs were purified from free lipids or MSP using SEC on Waters H-class using an in-house packed column packed with Superdex 200 prep-grade beads (300 × 7.8 mm) in 20 mM HEPES pH 7.2 (Cytiva, cat no. 17-1043-01). Protein standards (Biorad, cat no.1511901) were used to evaluate the separation of the in-house column (Figure S8) at a flow rate of 1 mL/min. Nanodisc were purified at a flow rate of 0.5 mL/min. Fraction volumes of 0.5 mL were collected, and 12.5% SDS-PAGE gels were used to confirm that fractions contained MSP. Fractions that contained MSP were collected and concentrated to 150−300 uM with 20% D_2O final concentrations for NMR verification.

Nanodisc verifications were acquired on a Bruker DRX600 NMR spectrometer operated with XWINNMR software, version 3.5. The samples were prepared in a 3 mm NMR tube and acquired with a 5 mm broadband observe probe at 22 °C. The ^{1}H decoupled ^{31}P NMR spectra were acquired using a 30-degree 4.8-s pulse, 131,072 data points, and a relaxation delay of 0.1 s. The data was processed using a 2 Hz line broadening function. The instrument was calibrated using phosphoric acid and spectrum processed using TopSpin v4.1.3.

TRESI-HDX-MS of Cytochrome c Nanodisc Interactions. The complexes were assembled at a 1:1 molar ratio before TRESI-HDX-MS experiments, where the final concentration of cyt c was 5 uM in 20 mM HEPES at pH 7.2. The experimental setup design followed an established protocol with minor modifications.[31,32] The protein complex passes through the notched region of the inner capillary, mixing with D_2O in the outer capillary with a final concentration of 50% D_2O, for various time points. Before protease digestion, the labeled sample was quenched using 0.5% formic acid in water. The resulting peptides were desalted, trapped, and separated on an ACQUITY UPLC BEH C18 VanGuard Pre-column (Waters, MA). Eluted peptides were ionized by electrospray

https://doi.org/10.1021/jasms.4c00478
J. Am. Soc. Mass Spectrom. 2025, 36, 1052−1059

and detected using a Synapt G2S mass spectrometer (Waters, MA). The mass spectrometer was equipped with an IMS to provide additional peptide separation. An LC gradient from 5% to 35% 0.1% FA in acetonitrile was used to elute peptides for analysis, followed by a 15 min hold at 85% acetonitrile to elute trapped lipids between each injection. The generated peptides were identified using ProteinLynx Global Server (PLGS), Table S1. All time points were acquired in quadruplicate technical replicates.

RESULTS AND DISCUSSION

Verification of Nanodiscs Using Size-Exclusion Chromatography and NMR. The purification and verification of nanodiscs was conducted using size-exclusion chromatography (SEC), SDS-PAGE, and 1D 31P NMR. Figure 2A−D illustrates the UV280 trace of DMPC, POPG, CL, and DMPC:POPG, respectively, along with the SDS-PAGE bands corresponding to the MSP in specific fractions. Due to the heterogeneity of nanodisc assembly, SEC allowed for the initial evaluation of the preparation, where the chromatograms are normalized to the maximum peak intensity and the relative yield of nanodiscs compared to empty liposomes or lipid-free MSP. SDS-PAGE analysis of the SEC fractions reveals a protein band corresponding to MSP1D1 (~24 kDa) with high purity (Figure S1). In DMPC and POPG samples, the ratio between MSP and lipids resulted mainly in aggregation/liposomal formation in addition to nanodiscs, as confirmed by SEC.[33] Although aggregation/liposomes were found in the sample preparation, only fractions containing the highest concentration of MSP1D1 (with a retention time of ~14 min) were used in further analysis.

Interestingly, peaks of CL nanodiscs shift toward a shorter retention time compared to POPG nanodiscs, from which the CL phospholipid is derived.[6,34] Since the size of the nanodiscs is governed by the packing protein used in both cases (MSP1D1), this shift in retention may be a consequence of interactions between the agarose-dextran matrix of the column beads rather than a size difference.[35] Differences in retention times have been observed with different ratios of differently charged phospholipids,[36] but in this case these differences likely reflect different charge densities for "cylindrical" single tailed phopsholipids (POPG), and "conical" double tailed phopsholipids like CL, something that will come into play for nanodisc/cyt c interactions.[25,37,38] It is also a possibility that CL is forming nonconnonical nanodisc-like structures, for example with alternate MSP wrapping,[39] that have a larger average size than the canonical form.

Selected fractions from DMPC (14 min), POPG (14 min), and CL (11 min) nanodiscs were verified by using 1D 31P NMR (Figure S2). The presence of formed nanodiscs was characterized by a sharp peak around 0 ppm in each NMR spectrum. The NMR peaks produced from nanodiscs were compared to the NMR peaks produced from liposomes (Figure S2). These results correlated well with those of others who have previously confirmed the presence of nanodiscs using 31P NMR.[40−42]

The Cyt c Nanodisc Binding Interface. TRESI-HDX-MS was used to obtain conformational insight into the interactions between cyclic cation and various phospholipid headgroups in nanodiscs. As previously described, this method allows for insight into conformational dynamics with labeling times in the millisecond to second time regime, with the ability to detect both direct interactions and subtle changes in conformational dynamics due to complex formation.[26,43] TRESI-HDX is particularly useful in difference HDX measurements when the "bound" condition involves rapid cycling between "on" and "off" states, which is common for weak binding interactions (but, less appreciated, also quite possible for relatively "tight" binders if k_{on} and k_{off} are both high). This situation results in an early (ms to s timesccale) "time of maximum difference" between kinetic profiles arising from the bound and unbound conditions. While the kinetics and thermodynamics of the interactions between cyt c and nanodiscs have not been characterized, the low amplitude of our HDX difference data suggest a relatively weak interaction, and the early times of maximum difference support a fast-cycling one.

Sequence coverage of 87.6%, and 3.00 redundancy was achieved using an in-house NHS-pepsin column (Figure S3). These experiments included three time-points (0.5, 2, and 5 s) of four different protein states: cyt c alone, cyt c with 10 nm DMPC nanodiscs, cyt c with 10 nm POPG nanodiscs, and cyt c with 10 nm CL nanodiscs. Figure 3A−D bar plots illustrate the summed difference in deuterium uptake between bound cyt c and free cyt c, integrated over 3 time points (each of which was measured in quadruplicate, Figures S4−S7). These differences are mapped onto the 1HRC PDB structure for POPG and CL nanodiscs in Figure 3E,F. The observed HDX differences are small, suggesting a relatively weak and dynamic interaction, but they are reproducible, consistently independently measured in redundant peptides, and statistically significant (to 2σ, n = 4−12, Table S2). It is essential to note that these differences were observed for nanodiscs containing 100% anionic phospholipid (POPG and CL), but not for nanodiscs containing DMPC. This is expected, since DMPC is neutral, and it was used here as a negative control to determine if phospholipid or MSP affected the deuterium uptake of cyt c in the absence of significant specific interactions. Furthermore, in support of our findings, Imai et al. (2016) observed similar results when conducting paramagnetic-quench EPR experiments on horse heart cyt c, supporting the idea that other negatively charged lipids (specifically in their case DOPG) can elicit CL-like structural changes in cyt c.[44]

Upon complexation, significant deuterium uptake differences are observed in two regions of cyt c, corresponding to a.a. D2-F10 and M65-F82. These regions are exactly in agreement with the putative L and A binding sites, as proposed from various studies using NMR, FTIR, and MALDI-TOF.[3,5,6,18] In addition, Mohommadyani et al. (2018) provided evidence of simultaneous engagement of two binding sites, which overlapped mainly with the A- and L-sites using molecular docking, which was evaluated using solution NMR.[3] These two hydrophobic patches on the protein's surface may serve as a membrane anchor, as both domains are near lysine residues, providing additional electrostatic interactions with the phospholipid head groups (Figure 3E,F).[3,5] Importantly, in the presence of CL, HDX an additional decrease in uptake was observed in peptides F82-L94. Recently, Li et al. (2019) observed, using solid-state NMR, that upon complexation with LUVs containing CL, I81 and F82 induce spectral changes.[45] Furthermore, dynamic changes in the residues N70−I85 loop have been reported as a selectivity for CL.[45]

Conformational Restructuring of Cyt c upon Complexation. Apart from the sites of initial interaction, there has been extensive debate about the nature (or occurrence) of substantial structural changes in cyt c upon complexation.

https://doi.org/10.1021/jasms.4c00478
J. Am. Soc. Mass Spectrom. 2025, 36, 1052−1059

Multiple groups have observed significant differences in cyt c structure in the presence of phospholipids and attributed them to tertiary structural changes of the protein upon binding.[1,4,6,7,46] It remains to be seen if the observed tertiary structural changes are due to a large [cyt c]/[CL] ratio[16] or perhaps crowding of cyt c on the membrane surface, as this ensemble is challenging to probe.[6] The current published literature has shown that two distinct types of CL-bound cyt c conformations can be observed: a largely unfolded one and another with native-like compactness.[46,47] However, others have provided evidence that cyt c upon CL-binding remains unaltered. Wand and collaborators provided evidence using reverse lipid micelles by NMR to show that upon binding to CL phospholipid, cyt c remains unaltered.[48] This latter model is in line with our HDX data, which provide no evidence of significant unfolding of cyt c upon complexation.

Other research groups have also provided evidence of this using different methods like HSQC (NMR), and the structural conformation of cyt c in the presence and absence of vesicles overlapped quite well.[49] Solid-state NMR showed that in the presence of DOPC/CL unilamellar vesicles, the cyt c/CL complex promoted peroxidase activity without substantially affecting the 31P or the 13C frequencies of the lipid glycerol signals.[49] This further supports our data that cyt c in the presence of CL phospholipids remains largely structurally unaltered.

It was not until recently that various research groups, such as Ripanti et al. (2021), provided evidence against the lipid anchorage model.[16] Their study using Attenuated Total Reflection InfraRed spectroscopy (ATR-IR) and Fluorescence Resonance Energy Transfer (FRET) experiments concluded that there was no evidence of the insertion of a lipid acyl chain in the cyt c hydrophobic core. Instead, the insertion occurred only when the ratio of [Cyt c]/[CL lipids] exceeded 0.15. CD measurements also supported this finding where evidence of tertiary structural changes was observed on the protein when the ratio of [Cyt c]/[CL lipids] was more significant than 0.2.[16,46] Therefore, it remains unclear whether the structural differences observed are related to the experimental conditions or methods used. It is also hard to determine if liposomes are biologically relevant in understanding the structural dynamics of cyt c in the presence of CL because various groups have determined tertiary unfolding while others using similar methods showed no differences.[47] Furthermore, some have attempted to use molecular modeling to manually dock one or two acyl chains into the heme moiety. Still, results demand a substantial conformational change to provide a channel where the acyl chain may be lodged.[50,51] Ultimately, our HDX data do not support a substantial degree of lipid anchorage even for 100% CL nanodiscs.

Mixed Lipid Nanodiscs. It can be argued that the conformational changes observed in 100% CL nanodiscs are not representative of the mitochondrial membrane and can drive nonphysiological conformational changes of cyt c. In mitochondria, CL phospholipids typically represent between 5 and 20% of the total lipid content of the inner membrane; therefore, producing nanodiscs that contained 80% DMPC and 20% CL would be ideal. However, after various attempts, we were not successful in making multicomplex nanodiscs with DMPC and CL.[6] This could be due to the differences in sample preparation using the two different lipids. We were able to generate nanodiscs using an 80:20 DMPC:POPG ratio; however, we were unable to detect binding to these nanodiscs (Figure 3D), which may result from strongly favored incorporation of DMPC during reconstitution, or simply binding below our threshold of detection. Nonetheless, our data suggest that the general features of cyt c membrane interactions—interactions at the A- and L- sites, without a substantial subsequent conformational change—are retained for different negatively charged phospholipids, so that even pure POPG nanodiscs can serve as a reasonable in vitro model for cyt c membrane interactions.

CONCLUSIONS

Cyt c exhibits great functional complexity despite being a small protein with a relatively simple global fold. Here, we have provided evidence regarding the interaction of cyt c with flat-structured nanodisc membrane mimics. In HDX, the membrane-bound protein reveals aspects of the initial membrane interaction through the proposed A-site and L-site under physiological pH conditions. Further characterization of the dynamics of cyt c in the presence of CL compositions, such as tetra-stearyl-cardiolipin[22] and tetra-myristoyl-cardiolipin,[21] embedded nanodiscs is required, as the affinity of cyt c to these lipids differ and correlates to its peroxidase activities. In addition to the presence of H_2O_2, such studies provide a better understanding of the mechanism required to release cyt c during the early stages of apoptosis. It may support further development of therapeutic approaches.

ASSOCIATED CONTENT

Supporting Information

The Supporting Information is available free of charge at https://pubs.acs.org/doi/10.1021/jasms.4c00478.

Representative SDS-PAGE for the fractions collected via SEC during the purification (Figure 1S); 1D 31P nuclear magnetic resonance spectra of nanodiscs (Figure S2); % sequence coverage and redundancy (Figure S3); Cyt c peptide list (Table S1); raw deuterium uptake kinetic plots (Figures S4−S7); HDX summary table (Table S2); size exclusion chromatogram of protein standard using in-house packed column (Figure S8) (PDF)

AUTHOR INFORMATION

Corresponding Author

Derek J. Wilson − *Department of Chemistry, York University, Toronto, Ontario M3J 1P3, Canada;* orcid.org/0000-0002-7012-6085; Phone: +1-416-736-2100; Email: dkwilson@yorku.ca

Authors

Vimanda Chow − *Department of Chemistry, York University, Toronto, Ontario M3J 1P3, Canada*

Cristina Lento − *Department of Chemistry, York University, Toronto, Ontario M3J 1P3, Canada*

Complete contact information is available at: https://pubs.acs.org/10.1021/jasms.4c00478

Author Contributions

The manuscript was written through contributions of all authors. All authors have given approval to the final version of the manuscript.

Notes

The authors declare no competing financial interest.

■ ACKNOWLEDGMENTS

This work was funded by the Natural Sciences and Engineering Research Council of Canada Discovery Grant (RGPIN 480432) and Collaborative Research and development Grant (CRD-PJ 58776)

■ REFERENCES

(1) Schweitzer-Stenner, R. Relating the Multi-Functionality of Cytochrome c to Membrane Binding and Structural Conversion. *Biophys. Rev.* **2018**, *10* (4), 1151−1185.
(2) Kagan, V. E.; Bayir, H. A.; Belikova, N. A.; Kapralov, O.; Tyurina, Y. Y.; Tyurin, V. A.; Jiang, J.; Stoyanovsky, D. A.; Wipf, P.; Kochanek, P. M.; Greenberger, J. S.; Pitt, B.; Shvedova, A. A.; Borisenko, G. Cytochrome c/Cardiolipin Relations in Mitochondria: A Kiss of Death. *Free Radic. Biol. Med.* **2009**, *46* (11), 1439−1453.
(3) Mohammadyani, D.; Yanamala, N.; Samhan-Arias, A. K.; Kapralov, A. A.; Stepanov, G.; Nuar, N.; Planas-Iglesias, J.; Sanghera, N.; Kagan, V. E.; Klein-Seetharaman, J. Structural Characterization of Cardiolipin-Driven Activation of Cytochrome c into a Peroxidase and Membrane Perturbation. *Biochim. Biophys. Acta BBA - Biomembr.* **2018**, *1860* (5), 1057−1068.
(4) Heimburg, T.; Marsh, D. Investigation of Secondary and Tertiary Structural Changes of Cytochrome c in Complexes with Anionic Lipids Using Amide Hydrogen Exchange Measurements: An FTIR Study. *Biophys. J.* **1993**, *65* (6), 2408−2417.
(5) Oellerich, S.; Lecomte, S.; Paternostre, M.; Heimburg, T.; Hildebrandt, P. Peripheral and Integral Binding of Cytochrome c to Phospholipids Vesicles. *J. Phys. Chem. B* **2004**, *108* (12), 3871−3878.
(6) Díaz-Quintana, A.; Pérez-Mejías, G.; Guerra-Castellano, A.; De La Rosa, M. A.; Díaz-Moreno, I. Wheel and Deal in the Mitochondrial Inner Membranes: The Tale of Cytochrome *c* and Cardiolipin. *Oxid. Med. Cell. Longev.* **2020**, *2020*, 1−20.
(7) Elmer-Dixon, M. M.; Xie, Z.; Alverson, J. B.; Priestley, N. D.; Bowler, B. E. Curvature-Dependent Binding of Cytochrome *c* to Cardiolipin. *J. Am. Chem. Soc.* **2020**, *142* (46), 19532−19539.
(8) Fiorucci, L.; Erba, F.; Santucci, R.; Sinibaldi, F. Cytochrome c Interaction with Cardiolipin Plays a Key Role in Cell Apoptosis: Implications for Human Diseases. *Symmetry* **2022**, *14* (4), 767.
(9) Muenzner, J.; Toffey, J. R.; Hong, Y.; Pletneva, E. V. Becoming a Peroxidase: Cardiolipin-Induced Unfolding of Cytochrome c. *J. Phys. Chem. B* **2013**, *117* (42), 12878−12886.
(10) Garrido, C.; Galluzzi, L.; Brunet, M.; Puig, P. E.; Didelot, C.; Kroemer, G. Mechanisms of Cytochrome c Release from Mitochondria. *Cell Death Differ.* **2006**, *13* (9), 1423−1433.
(11) Santucci, R.; Sinibaldi, F.; Cozza, P.; Polticelli, F.; Fiorucci, L. Cytochrome c: An Extreme Multifunctional Protein with a Key Role in Cell Fate. *Int. J. Biol. Macromol.* **2019**, *136*, 1237−1246.
(12) Pandiscia, L. A.; Schweitzer-Stenner, R. Coexistence of Native-like and Non-Native Partially Unfolded Ferricytochrome c on the Surface of Cardiolipin-Containing Liposomes. *J. Phys. Chem. B* **2015**, *119* (4), 1334−1349.
(13) Barayeu, U.; Lange, M.; Méndez, L.; Arnhold, J.; Shadyro, O. I.; Fedorova, M.; Flemmig, J. Cytochrome c Autocatalyzed Carbonylation in the Presence of Hydrogen Peroxide and Cardiolipins. *J. Biol. Chem.* **2019**, *294* (6), 1816−1830.
(14) Rytömaa, M.; Kinnunen, P. K. Evidence for Two Distinct Acidic Phospholipid-Binding Sites in Cytochrome c. *J. Biol. Chem.* **1994**, *269* (3), 1770−1774.
(15) Sinibaldi, F.; Howes, B. D.; Droghetti, E.; Polticelli, F.; Piro, M. C.; Di Pierro, D.; Fiorucci, L.; Coletta, M.; Smulevich, G.; Santucci, R. Role of Lysines in Cytochrome c−Cardiolipin Interaction. *Biochemistry* **2013**, *52* (26), 4578−4588.
(16) Ripanti, F.; Di Venere, A.; Cestelli Guidi, M.; Romani, M.; Filabozzi, A.; Carbonaro, M.; Piro, M. C.; Sinibaldi, F.; Nucara, A.; Mei, G. The Puzzling Problem of Cardiolipin Membrane-Cytochrome c Interactions: A Combined Infrared and Fluorescence Study. *Int. J. Mol. Sci.* **2021**, *22* (3), 1334.
(17) Tuominen, E. K. J.; Wallace, C. J. A.; Kinnunen, P. K. J. Phospholipid-Cytochrome c Interaction. *J. Biol. Chem.* **2002**, *277* (11), 8822−8826.
(18) Kawai, C.; Prado, F. M.; Nunes, G. L. C.; Mascio, P. D.; Carmona-Ribeiro, A. M.; Nantes, I. L. pH-Dependent Interaction of Cytochrome c with Mitochondrial Mimetic Membranes: THE ROLE OF AN ARRAY OF POSITIVELY CHARGED AMINO ACIDS *. *J. Biol. Chem.* **2005**, *280* (41), 34709−34717.
(19) Milorey, B.; Schweitzer-Stenner, R.; Kurbaj, R.; Malyshka, D. pH-Induced Switch between Different Modes of Cytochrome *c* Binding to Cardiolipin-Containing Liposomes. *ACS Omega* **2019**, *4* (1), 1386−1400.
(20) Reis, R. I.; Moraes, I. Probing Membrane Protein Assembly into Nanodiscs by In Situ Dynamic Light Scattering: A2A Receptor as a Case Study. *Biology* **2020**, *9* (11), 400.
(21) Belikova, N. A.; Vladimirov, Y. A.; Osipov, A. N.; Kapralov, A. A.; Tyurin, V. A.; Potapovich, M. V.; Basova, L. V.; Peterson, J.; Kurnikov, I. V.; Kagan, V. E. Peroxidase Activity and Structural Transitions of Cytochrome c Bound to Cardiolipin-Containing Membranes. *Biochemistry* **2006**, *45* (15), 4998−5009.
(22) Abe, M.; Niibayashi, R.; Koubori, S.; Moriyama, I.; Miyoshi, H. Molecular Mechanisms for the Induction of Peroxidase Activity of the Cytochrome c−Cardiolipin Complex. *Biochemistry* **2011**, *50* (39), 8383−8391.
(23) Kyaw, A.; Roepke, K.; Arthur, T.; Howard, K. P. Conformation of Influenza AM2Membrane Protein in Nanodiscs and Liposomes. *Biochim. Biophys. Acta BBA - Biomembr.* **2023**, *1865* (5), 184152.
(24) Sanders, H. M.; Kostelic, M. M.; Zak, C. K.; Marty, M. T. Lipids and EGCG Affect α-Synuclein Association and Disruption of Nanodiscs. *Biochemistry* **2022**, *61* (11), 1014−1021.
(25) Gasanoff, E. S.; Yaguzhinsky, L. S.; Garab, G. Cardiolipin, Non-Bilayer Structures and Mitochondrial Bioenergetics: Relevance to Cardiovascular Disease. *Cells* **2021**, *10* (7), 1721.
(26) Chow, V.; Wolf, E.; Lento, C.; Wilson, D. J. Developments in Rapid Hydrogen−Deuterium Exchange Methods. *Essays Biochem.* **2023**, *67* (2), 165−174.
(27) Oganesyan, I.; Lento, C.; Wilson, D. J. Contemporary Hydrogen Deuterium Exchange Mass Spectrometry. *Methods* **2018**, *144*, 27−42.
(28) Sligar, S. G.; Denisov, I. G. Nanodiscs: A Toolkit for Membrane Protein Science. *Protein Sci. Publ. Protein Soc.* **2021**, *30* (2), 297−315.
(29) Bayburt, T. H.; Grinkova, Y. V.; Sligar, S. G. Self-Assembly of Discoidal Phospholipid Bilayer Nanoparticles with Membrane Scaffold Proteins. *Nano Lett.* **2002**, *2* (8), 853−856.
(30) Fox, C. A.; Romenskaia, I.; Dagda, R. K.; Ryan, R. O. Cardiolipin Nanodisks Confer Protection against Doxorubicin-Induced Mitochondrial Dysfunction. *Biochim. Biophys. Acta BBA - Biomembr.* **2022**, *1864* (10), 183984.
(31) Wolf, E.; Lento, C.; Pu, J.; Dickinson, B. C.; Wilson, D. J. Innate Conformational Dynamics Drive Binding Specificity in Anti-Apoptotic Proteins Mcl-1 and Bcl-2. *Biochemistry* **2023**, *62* (11), 1619−1630.
(32) Oganesyan, I.; Lento, C.; Tandon, A.; Wilson, D. J. Conformational Dynamics of α-Synuclein during the Interaction with Phospholipid Nanodiscs by Millisecond Hydrogen−Deuterium Exchange Mass Spectrometry. *J. Am. Soc. Mass Spectrom.* **2021**, *32* (5), 1169−1179.
(33) Mabrouk, M. T.; Zidan, A. A.; Aly, N.; Mohammed, M. T.; Ghantous, F.; Seaman, M. S.; Lovell, J. F.; Nasr, M. L. Circularized Nanodiscs for Multivalent Mosaic Display of SARS-CoV-2 Spike Protein Antigens. *Vaccines* **2023**, *11* (11), 1655.
(34) Schlame, M. Thematic Review Series: Glycerolipids. Cardiolipin Synthesis for the Assembly of Bacterial and Mitochondrial Membranes. *J. Lipid Res.* **2008**, *49* (8), 1607−1620.
(35) Lundqvist, J. *Size Exclusion Chromatography*. Cytiva. https://www.cytivalifesciences.com/en/us/solutions/protein-research/knowledge-center/protein-purification-methods/size-exclusion-chromatography (accessed 2024-04-07).

https://doi.org/10.1021/jasms.4c00478
J. Am. Soc. Mass Spectrom. 2025, 36, 1052−1059

(36) Wadsäter, M.; Maric, S.; Simonsen, J.; Mortensen, K.; Cárdenas, M. The Effect of Using Binary Mixtures of Zwitterionic and Charged Lipids on Nanodisc Formation and Stability. *Soft Matter* **2013**, *9*, 2329−2337.
(37) Ikon, N.; Ryan, R. O. Cardiolipin and Mitochondrial Cristae Organization. *Biochim. Biophys. Acta BBA - Biomembr.* **2017**, *1859* (6), 1156−1163.
(38) Dickey, A.; Faller, R. Examining the Contributions of Lipid Shape and Headgroup Charge on Bilayer Behavior. *Biophys. J.* **2008**, *95* (6), 2636−2646.
(39) Dalal, V.; Arcario, M. J.; Petroff, J. T.; Tan, B. K.; Dietzen, N. M.; Rau, M. J.; Fitzpatrick, J. A. J.; Brannigan, G.; Cheng, W. W. L. Lipid Nanodisc Scaffold and Size Alter the Structure of a Pentameric Ligand-Gated Ion Channel. *Nat. Commun.* **2024**, *15*, 25.
(40) Krishnarjuna, B.; Ravula, T.; Ramamoorthy, A. Detergent-Free Isolation of CYP450-Reductase's FMN-Binding Domain in E. Coli Lipid-Nanodiscs Using a Charge-Free Polymer. *Chem. Commun.* **2022**, *58* (31), 4913−4916.
(41) Ravula, T.; Ramadugu, S. K.; Di Mauro, G.; Ramamoorthy, A. Bioinspired, Size-Tunable Self-Assembly of Polymer-Lipid Bilayer Nanodiscs. *Angew. Chem., Int. Ed. Engl.* **2017**, *56* (38), 11466−11470.
(42) Ravula, T.; Sahoo, B. R.; Dai, X.; Ramamoorthy, A. Natural-Abundance ^{17}O NMR Spectroscopy of Magnetically Aligned Lipid Nanodiscs. *Chem. Commun.* **2020**, *56* (69), 9998−10001.
(43) Anacleto, J.; Lento, C.; Sarpe, V.; Maqsood, A.; Mehrazma, B.; Schriemer, D.; Wilson, D. J. Apparatus for Automated Continuous Hydrogen Deuterium Exchange Mass Spectrometry Measurements from Milliseconds to Hours. *Anal. Chem.* **2023**, *95* (9), 4421−4428.
(44) Imai, M.; Saio, T.; Kumeta, H.; Uchida, T.; Inagaki, F.; Ishimori, K. Investigation of the Redox-Dependent Modulation of Structure and Dynamics in Human Cytochrome c. *Biochem. Biophys. Res. Commun.* **2016**, *469* (4), 978−984.
(45) Li, M.; Mandal, A.; Tyurin, V. A.; DeLucia, M.; Ahn, J.; Kagan, V. E.; van der Wel, P. C. A. Surface-Binding to Cardiolipin Nanodomains Triggers Cytochrome *c* Pro-Apoptotic Peroxidase Activity via Localized Dynamics. *Structure* **2019**, *27* (5), 806−815.e4.
(46) Hong, Y.; Muenzner, J.; Grimm, S. K.; Pletneva, E. V. Origin of the Conformational Heterogeneity of Cardiolipin-Bound Cytochrome c. *J. Am. Chem. Soc.* **2012**, *134* (45), 18713−18723.
(47) Serpas, L.; Milorey, B.; Pandiscia, L. A.; Addison, A. W.; Schweitzer-Stenner, R. Autoxidation of Reduced Horse Heart Cytochrome c Catalyzed by Cardiolipin-Containing Membranes. *J. Phys. Chem. B* **2016**, *120* (48), 12219−12231.
(48) O'Brien, E. S.; Nucci, N. V.; Fuglestad, B.; Tommos, C.; Wand, A. J. Defining the Apoptotic Trigger. *J. Biol. Chem.* **2015**, *290* (52), 30879−30887.
(49) Mandal, A.; Hoop, C. L.; DeLucia, M.; Kodali, R.; Kagan, V. E.; Ahn, J.; van der Wel, P. C. A. Structural Changes and Proapoptotic Peroxidase Activity of Cardiolipin-Bound Mitochondrial Cytochrome c. *Biophys. J.* **2015**, *109* (9), 1873−1884.
(50) Sinibaldi, F.; Howes, B. D.; Piro, M. C.; Polticelli, F.; Bombelli, C.; Ferri, T.; Coletta, M.; Smulevich, G.; Santucci, R. Extended Cardiolipin Anchorage to Cytochrome c: A Model for Protein-Mitochondrial Membrane Binding. *J. Biol. Inorg. Chem. JBIC Publ. Soc. Biol. Inorg. Chem.* **2010**, *15* (5), 689−700.
(51) Dickerson, R. E.; Takano, T.; Eisenberg, D.; Kallai, O. B.; Samson, L.; Cooper, A.; Margoliash, E. Ferricytochrome c. *J. Biol. Chem.* **1971**, *246* (5), 1511−1535.

https://doi.org/10.1021/jasms.4c00478
J. Am. Soc. Mass Spectrom. 2025, 36, 1052−1059